DALTON
FULL PAPER

Synthesis, structural relationships and magnetic properties of new amine-templated manganese(II) phosphate oxalate framework materials

Zoe A. D. Lethbridge,[a] Satish K. Tiwary,[b] Andrew Harrison[b] and Philip Lightfoot*[a]

[a] *School of Chemistry, University of St Andrews, North Haugh, St Andrews, Fife, UK KY16 9ST. E-mail: pl@st-andrews.ac.uk*
[b] *Department of Chemistry, University of Edinburgh, The King's Buildings, West Mains Road, Edinburgh, UK EH9 3JJ*

Received 30th January 2001, Accepted 3rd May 2001
First published as an Advance Article on the web 29th May 2001

Three novel three-dimensional framework materials in the manganese(II)–phosphate–oxalate system have been prepared hydrothermally using organic amines as structure-directing agents. $[H_3NC_6H_{10}NH_3][Mn_2(HPO_4)_2(C_2O_4)(H_2O)_2]$ **1** and $[H_3N(CH_2)_2NH_3][Mn_2(HPO_4)_2(C_2O_4)(H_2O)_2]$ **2** have related, but not isomorphous, structures based on layers of vertex-sharing MnO_6 and PO_4 polyhedra linked by bridging oxalate groups. $[H_3N(CH_2)_2NH_3][Mn_4(HPO_4)_2(C_2O_4)_3(H_2O)_2]\cdot 2H_2O$ **3** has a very different structure composed of edge-sharing dimeric MnO_6 units linked into chains by PO_4 groups, and into a 3-D framework by oxalate units. **3** can be topotactically dehydrated, with loss of both extra-framework and co-ordinated water, to produce a new phase **4**. The magnetic susceptibilities of phases **1**, **3** and **4** all show Curie–Weiss behaviour above about 50 K, and a maximum in the susceptibility curve in the vicinity of 7–12 K, indicating significant antiferromagnetic exchange. Structural relationships to other phosphate–oxalate frameworks are discussed.

Introduction

The application of solution-based or hydrothermal techniques to the synthesis of new inorganic materials has grown enormously in the last few years.[1] Particular emphasis has been placed on the use of organic 'structure-directing agents' (SDAs), the original purpose of which was to act as a 'template' around which a new framework may form, with subsequent thermal or chemical removal of the template producing a genuinely 'microporous' material, for future guest incorporation. However, in a much wider sense the use of an SDA for reasons other than templating is a field which as yet has not been explored greatly. The presence of the SDA will most often lead to framework topologies which would otherwise be inaccessible without the SDA, or with an SDA of a different size, shape or chemical nature. It is clear that judicious use of the SDA may eventually lead to the rational design of new framework topologies which may have tailored connectivities between appropriate 'active' framework sites to give specific physical or chemical properties, a particular example being the design of new magnetic materials with the framework metal–metal interactions to some extent governed by the requirements of the SDA. For example, several materials of the type $A[M^{II}M'^{III}(C_2O_4)_3]$ have been reported, where M^{II} = Mn or Fe, M'^{III} = Cr or Fe and A is a cation, most often of the form XR_4^+ (X = N or P).[2–7] These materials adopt layered structures based on a 'honeycomb-like' hexagonal grid of oxalate-linked M and M′ octahedra. The A cations are found between the layers, and are used to control the stacking and spacing of the layers;[6] however whilst the near-neighbour magnetic exchange depends on M and M′, the nature of A affects the overall magnetic ordering. Thus, in the ferromagnetic series $N(n\text{-}C_nH_{2n+1})_4Fe^{II}Fe^{III}(C_2O_4)_3$ (n = 3–5), as n increases (leading to an increase in the interlayer spacing) the values of θ and T_c also increase.[4]

It is now clear that new frameworks may be synthesized by variation not only of SDAs but also by the introduction of new combinations of framework building units. The use of mixed anions, for example phosphate and oxalate, has recently led to the synthesis of several new materials by ourselves and others, *e.g.* $[NH_3(CH_2)_2NH_3]_{2.5}[Al_4H(HPO_4)_4(H_2PO_4)_2(C_2O_4)_4]$,[8] $[Fe_4(PO_4)_2(C_2O_4)(H_2O)_2]$,[9] $[Mn_4(PO_4)_2(C_2O_4)(H_2O)_2]$ and $[H_3N(CH_2)_3NH_3][Mn_2(HPO_4)_2(C_2O_4)(H_2O)_2]$,[10] $[NH_3(CH_2)_2NH_3]_{1.5}[Fe_3(PO_4)(HPO_4)_3(C_2O_4)_{1.5}]$,[11] $[C_{10}N_4H_{28}][Fe_2(HPO_4)_3(C_2O_4)]_2$[12] and $K_2[Ga_4(C_2O_4)(PO_4)_4]\cdot 2H_2O$.[13]

Our present goal, therefore, is to explore the hydrothermal chemistry of some of these new mixed anion systems, with a view to understanding the effects of different structure-directing agents and other synthetic variables on the framework topologies produced; its effect on the resultant magnetic properties, and also the possible effects of other structural features, for example the influence of 'zeolitic' water. Here we report the synthesis, structure and magnetic properties of three new manganese(II) phosphate oxalates, $[H_3NC_6H_{10}NH_3][Mn_2(HPO_4)_2(C_2O_4)(H_2O)_2]$ **1**, $[H_3N(CH_2)_2NH_3][Mn_2(HPO_4)_2(C_2O_4)(H_2O)_2]$ **2** and $[H_3N(CH_2)_2NH_3][Mn_4(HPO_4)_2(C_2O_4)_3(H_2O)_2]\cdot 2H_2O$ **3**.

Experimental

Synthesis of $[H_3NC_6H_{10}NH_3][Mn_2(HPO_4)_2(C_2O_4)(H_2O)_2]$ 1

$MnC_2O_4\cdot 2H_2O$ (3.2399 g, 18.1 mmol) was added to water (135 ml) with stirring, followed by addition of H_3PO_4(aq) (85%, 2.07 ml, 17.9 mmol). A 15 ml portion of this mixture was placed in a Teflon lined stainless steel autoclave (50 ml volume, corresponding to 30% filling) with *trans*-1,4-diaminocyclohexane (0.2307 g, 2.02 mmol) to give an approximate ratio of $MnC_2O_4\cdot 2H_2O$: H_3PO_4(aq) : $H_2NC_6H_{10}NH_2$: water 1 : 1 : 1 : 417. The mixture was heated at 120 °C for 48 hours, cooled in air, filtered and washed with distilled water and air dried. 0.4255 g of a pink/grey material was obtained, 78.1% yield on Mn. Found C, 20.16; H, 3.60; N, 5.09. $[H_3NC_2H_{10}NH_3][Mn_2(HPO_4)_2(C_2O_4)(H_2O)_2]$ requires C, 17.73; H, 4.09; N, 5.17%. A sample of **1** judged to be phase-pure by X-ray powder diffraction was prepared by sonication of the raw product.

 DOI: 10.1039/b101005k

Table 1 Crystal data and details of structure solution and refinement

	1	2	3
Formula	$[H_3NC_6H_{10}NH_3][Mn_2(HPO_4)_2(C_2O_4)(H_2O)_2]$	$[H_3N(CH_2)_2NH_3][Mn_2(HPO_4)_2(C_2O_4)(H_2O)_2]$	$[H_3N(CH_2)_2NH_3][Mn_4(HPO_4)_2(C_2O_4)_3(H_2O)_2]\cdot 2H_2O$
Formula weight	540.08	488.00	401.95
Crystal system	Monoclinic	Monoclinic	Triclinic
Space group	$P2_1/n$	$P2_1/n$	$P\bar{1}$
a/Å	5.9778(3)	5.4573(4)	7.830(4)
b/Å	16.6747(8)	8.9650(7)	8.041(4)
c/Å	8.4660(4)	15.253(1)	9.652(7)
α/°			76.29(5)
β/°	90.384(1)	98.924(1)	78.47(6)
γ/°			86.36(6)
V/Å^3	843.85(6)	737.22(8)	578.4(6)
Z	2	2	2
μ(Mo-Kα)/cm^{-1}	1.767	2.010	2.389
Total reflections	1272	1136	1637
Observed reflections ($I > 3\sigma(I)$)	883	808	1343
R, R_w	0.0299, 0.0333	0.0239, 0.0270	0.0305, 0.0390

This pure sample was used for subsequent magnetic charaterisation.

Synthesis of $[H_3N(CH_2)_2NH_3][Mn_2(HPO_4)_2(C_2O_4)(H_2O)_2]$ 2 and $[H_3N(CH_2)_2NH_3][Mn_4(HPO_4)_2(C_2O_4)_3(H_2O)_2]\cdot 2H_2O$ 3

$MnC_2O_4\cdot 2H_2O$ (3.2399 g, 18.1 mmol) was added to water (135 ml) with stirring, followed by addition of H_3PO_4(aq) (85%, 2.07 ml, 17.9 mmol). A 15 ml portion of this mixture was placed in a Teflon lined stainless steel autoclave with ethylenediamine (0.13 ml, 1.94 mmol) to give an approximate ratio $MnC_2O_4\cdot 2H_2O$: H_3PO_4(aq) : $H_2N(CH_2)_2NH_2$: water 1 : 1 : 1 : 417. The autoclave was heated at 120 °C for 48 hours and cooled in air. The mixture was filtered and washed with distilled water, then air dried to give 0.3132 g of pale pink blocky crystals of **3**. Found: C, 12.11; H, 1.80; N, 3.54. $[H_3N(CH_2)_2NH_3][Mn_4(HPO_4)_2(C_2O_4)_3(H_2O)_2]\cdot 2H_2O$ requires C, 11.86; H, 2.49; N, 3.46%. $[H_3N(CH_2)_2NH_3][Mn_2(HPO_4)_2(C_2O_4)(H_2O)_2]$ **2** is formed as a minor impurity in this reaction. Sonication produces a pure sample of **3**, however pure **2** has not been obtained.

Characterisation

Single crystal X-ray data collection for **1**, **2** and **3** was carried out at 295 K on a Bruker SMART diffractometer with a CCD detector and Mo-Kα radiation. Structure solution and refinement were carried out using the SIR 92[14] and TEXSAN[15] program suites. Crystallographic details are given in Table 1. Hydrogen atoms in structures **1** and **2** were located and isotropically refined. For **3**, hydrogen atoms on the amine were geometrically fixed, however no hydrogens on the water could be located and geometric placement did not lead to a successful refinement.

CCDC reference numbers 157825–157827.

See http://www.rsc.org/suppdata/dt/b1/b101005k/ for crystallographic data in CIF or other electronic format.

Thermogravimetric analysis (TGA) was carried out on a TA Instruments SDT 2960 simultaneous DTA–TGA furnace, from room temperature to 600 or 800 °C at a heating rate of 10 °C min^{-1} under both nitrogen and oxygen. Magnetisation measurements were carried out on polycrystalline samples loaded into gelatine capsules using a Quantum Design MPMS$_2$ SQUID magnetometer with an applied field of 100 Oe over the temperature range 1.7 to 300 K. The data were corrected for the diamagnetic contribution of the sample holder.

Results

Descriptions of the structures

$[H_3NC_6H_{10}NH_3][Mn_2(HPO_4)_2(C_2O_4)(H_2O)_2]$. $[H_3NC_6H_{10}NH_3][Mn_2(HPO_4)_2(C_2O_4)(H_2O)_2]$ **1** is a three-dimensional manganese phosphate oxalate framework containing diprotonated *trans*-1,4-diaminocyclohexane cations. The framework is similar to that of $[H_3N(CH_2)_3NH_3][Mn_2(HPO_4)_2(C_2O_4)(H_2O)_2]$ previously reported by us,[10] though not isostructural. The basic building unit is shown in Fig. 1; selected bond lengths and angles are in Table 2.

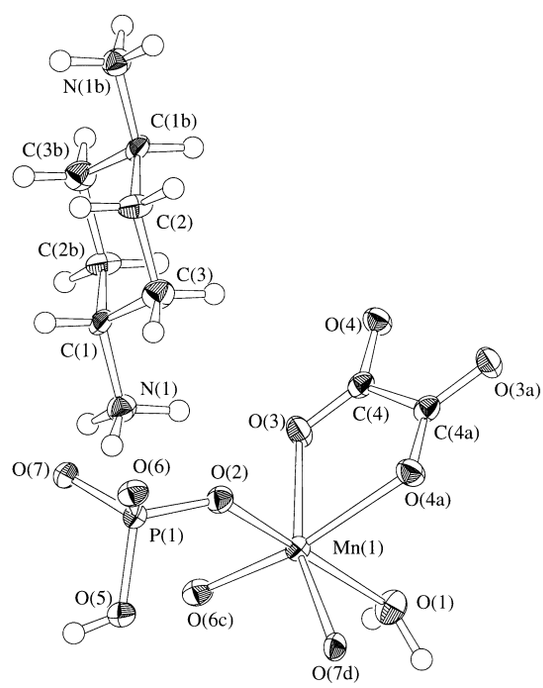

Fig. 1 Building unit of $[H_3NC_6H_{10}NH_3][Mn_2(HPO_4)_2(C_2O_4)(H_2O)_2]$ **1** showing the atom labelling scheme. Ellipsoids are shown at 50% probability. Symmetry labels: a, $-x+1$, $-y$, $-z+1$; b, $-x+2$, $-y$, $-z$; c, $x-1$, y, z; d, $x-\frac{1}{2}$, $-y+\frac{1}{2}$, $z+\frac{1}{2}$.

There is one crystallographically distinct manganese in the structure, which adopts distorted octahedral co-ordination, confirmed as Mn(II) by bond valence sums (Mn(1) 1.96).[16] The manganese co-ordination sphere consists of two oxalate oxygens, three phosphate oxygens and a water molecule. The smallest octahedral angle of 72.6(1)° is due to the bidentate oxalate co-ordination. The presence of the water molecule and also a hydroxyl group on the phosphate tetrahedron is indicated by the low bond valences of O(1) (0.28, H_2O) and O(5) (1.03, OH).

The framework is constructed from *cis* corner-sharing MnO_6–HPO_4 chains running along the *a* direction, which are

Table 2 Selected bond lengths (Å) and angles (°) in $[H_3NC_6H_{10}NH_3][Mn_2(HPO_4)_2(C_2O_4)(H_2O)_2]$ **1**

Mn(1)–O(1)	2.256(4)	Mn(1)–O(4)	2.279(4)
Mn(1)–O(2)	2.159(3)	Mn(1)–O(6)	2.169(3)
Mn(1)–O(3)	2.256(4)	Mn(1)–O(7)	2.128(3)
O(1)–Mn(1)–O(2)	90.5(1)	O(2)–Mn(1)–O(7)	95.0(1)
O(1)–Mn(1)–O(3)	90.5(1)	O(3)–Mn(1)–O(4)	72.6(1)
O(1)–Mn(1)–O(4)	82.2(1)	O(3)–Mn(1)–O(6)	161.9(1)
O(1)–Mn(1)–O(6)	83.9(1)	O(3)–Mn(1)–O(7)	94.3(1)
O(1)–Mn(1)–O(7)	172.8(1)	O(4)–Mn(1)–O(6)	89.6(1)
O(2)–Mn(1)–O(3)	87.8(1)	O(4)–Mn(1)–O(7)	94.1(1)
O(2)–Mn(1)–O(4)	158.9(1)	O(6)–Mn(1)–O(7)	89.9(1)
O(2)–Mn(1)–O(6)	109.4(1)		

A	H	B	A–H	H···B	A···B	A–H···B
O(1)	H(1)	O(2)	0.89(6)	1.99(6)	2.843(5)	161(6)
O(5)	H(3)	O(4)	0.72(6)	2.14(6)	2.793(5)	152(7)
N(1)	H(4)	O(7)	0.92(5)	1.98(5)	2.888(6)	170(4)
N(1)	H(5)	O(3)	0.93(6)	2.00(6)	2.882(6)	157(5)
N(1)	H(6)	O(6)	1.09(6)	1.88(6)	2.887(6)	151(5)
O(1)	H(1)	O(6)	0.89(6)	2.80(6)	3.087(5)	101(4)
N(1)	H(4)	O(4)	0.92(5)	2.81(4)	3.162(6)	104(3)
N(1)	H(4)	O(2)	0.92(5)	2.89(4)	3.220(5)	113(3)

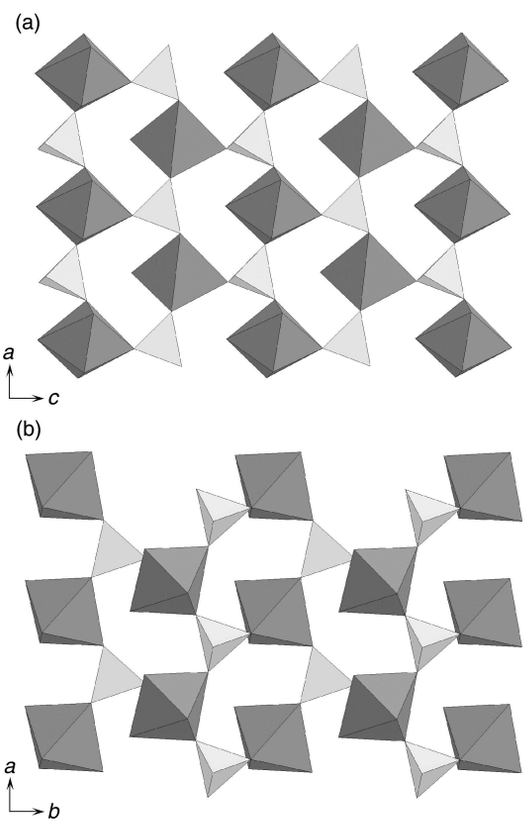

Fig. 2 Projection of the manganese phosphate layer in $[H_3NC_6H_{10}NH_3][Mn_2(HPO_4)_2(C_2O_4)(H_2O)_2]$ **1** (*a*) and $[H_3N(CH_2)_2NH_3][Mn_2(HPO_4)_2(C_2O_4)(H_2O)_2]$ **2** (*b*). MnO_6 dark grey octahedra, PO_4 light grey tetrahedra.

linked to each other *via* corner sharing HPO_4 tetrahedra to form layers in the *ac* plane (Fig. 2(a)). Each layer contains chains 'pointing' up and down, which alternate along the *c* direction. Oxalate anions co-ordinated to an 'up' chain connect one layer to the layer above, those co-ordinated to a 'down' chain to a layer below.

A *bc* projection (Fig. 3(a)) shows the full 3-D structure, with diprotonated *trans*-1,4-diaminocyclohexane cations in the channels along the *a* direction. Hydrogen bonding occurs between the amine and the framework oxygens (see Table 2).

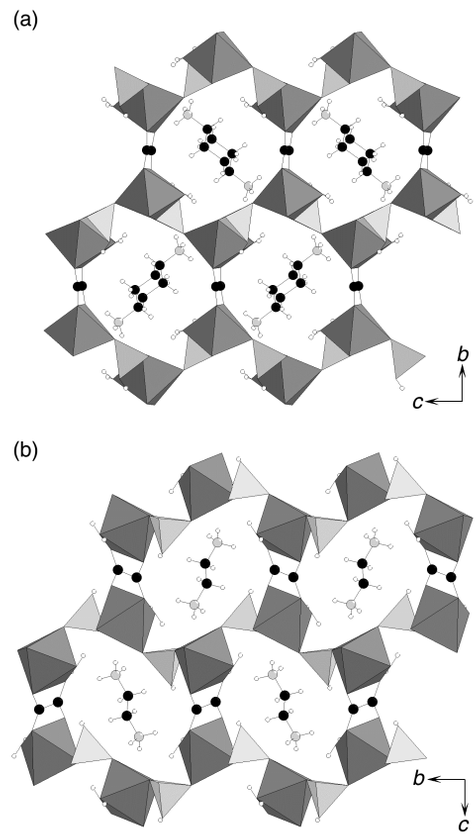

Fig. 3 **1** (*a*) and **2** (*b*) showing oxalate pillars and channels containing protonated cation. MnO_6 dark grey octahedra, PO_4 light grey tetrahedra, C black, N light grey, H white.

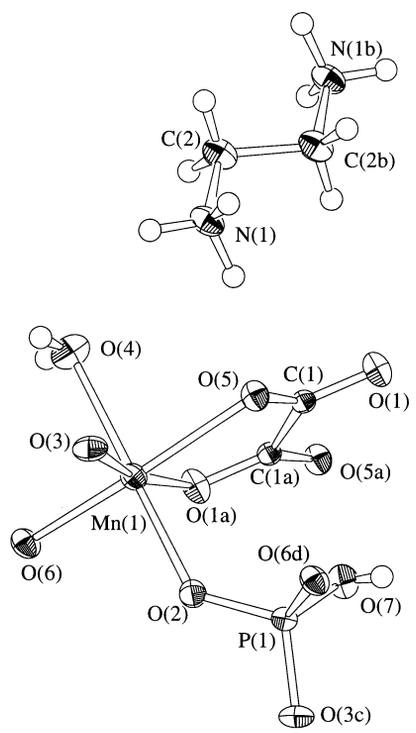

Fig. 4 Building unit of **2** showing the atom labelling scheme. Ellipsoids are shown at 50% probability. Symmetry labels: a, $-x$, $-y+1$, $-z+2$; b, $-x$, $-y+2$, $-z+2$; c, $-x-\frac{1}{2}$, $y-\frac{1}{2}$, $-z+\frac{3}{2}$; d, $x-1$, y, z.

$[H_3N(CH_2)_2NH_3][Mn_2(HPO_4)_2(C_2O_4)(H_2O)_2]$ 2. The building unit of **2** is shown in Fig. 4; selected bond lengths and angles are shown in Table 3. Manganese is confirmed as 2+ by bond valence calculations (sum = 2.07). The presence of a water

Table 3 Selected bond lengths (Å) and angles (°) in $[H_3N(CH_2)_2NH_3][Mn_2(HPO_4)_2(C_2O_4)(H_2O)_2]$ **2**

Mn(1)–O(1)	2.249(3)	Mn(1)–O(4)	2.273(3)
Mn(1)–O(2)	2.125(3)	Mn(1)–O(5)	2.254(3)
Mn(1)–O(3)	2.123(3)	Mn(1)–O(6)	2.119(3)
O(1)–Mn(1)–O(2)	91.1(1)	O(2)–Mn(1)–O(6)	91.9(1)
O(1)–Mn(1)–O(3)	169.7(1)	O(3)–Mn(1)–O(4)	88.5(1)
O(1)–Mn(1)–O(4)	87.9(1)	O(3)–Mn(1)–O(5)	96.8(1)
O(1)–Mn(1)–O(5)	73.23(9)	O(3)–Mn(1)–O(6)	102.3(1)
O(1)–Mn(1)–O(6)	87.2(1)	O(4)–Mn(1)–O(5)	84.1(1)
O(2)–Mn(1)–O(3)	92.5(1)	O(4)–Mn(1)–O(6)	87.7(1)
O(2)–Mn(1)–O(4)	178.9(1)	O(5)–Mn(1)–O(6)	159.0(1)
O(2)–Mn(1)–O(5)	95.9(1)		

A	H	B	A–H	H···B	A···B	A–H···B
O(4)	H(1)	O(6)	0.73(6)	2.24(7)	2.811(5)	136(7)
O(4)	H(2)	O(5)	0.80(6)	2.04(6)	2.825(4)	168(6)
O(7)	H(9)	O(1)	0.68(9)	2.04(9)	2.691(5)	162(10)
N(1)	H(3)	O(6)	0.92(5)	1.96(5)	2.817(5)	155(4)
N(1)	H(4)	O(5)	0.99(6)	1.97(6)	2.932(5)	165(5)
N(1)	H(8)	O(3)	0.90(5)	1.87(5)	2.771(5)	173(4)
O(4)	H(1)	O(2)	0.73(6)	2.41(7)	3.022(4)	142(7)
N(1)	H(8)	O(2)	0.90(5)	2.79(5)	3.079(4)	100(3)

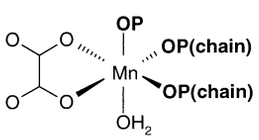

$[H_3NC_6H_{10}NH_3][Mn_2(HPO_4)_2(C_2O_4)(H_2O)_2]$

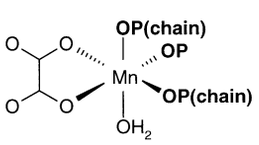

$[H_3N(CH_2)_2NH_3][Mn_2(HPO_4)_2(C_2O_4)(H_2O)_2]$

Fig. 5 Local co-ordination around the manganese octahedra in **1** and **2**.

(O(4)) and a hydroxyl group (O(7)) are also indicated by bond valence sums of 0.27 and 1.04 respectively. This material is isomorphous with the previously reported diaminopropane containing $[H_3N(CH_2)_3NH_3][Mn_2(HPO_4)_2(C_2O_4)(H_2O)_2]$[10] and will not be described in detail here. It displays similar connectivity to **1**, however the structures are quite different in appearance, as illustrated by a comparison of the layers in Fig. 2. Although **1** and **2** have the same *local* co-ordination around the Mn (*viz*. three HPO_4 groups in a *fac* configuration, a bidentate oxalate group and a terminal H_2O molecule), a difference in longer-range connectivity between the two can be seen. Although all phosphate tetrahedra are crystallographically equivalent, a distinction can be made between HPO_4 in one chain and HPO_4 in an adjacent one. The difference in connectivity of the chains is illustrated by the configuration of the MnO_6 octahedra in Fig. 5, where the 'chain' HPO_4 ligands are either *cis*/*trans* or *trans*/*trans* to the oxalate group. Fig. 3(b) shows a *bc* projection of **2**. The angle of the oxalate plane is noticeably different in the two structures. A similar material exists in the iron phosphate oxalate system, $[Fe_2(H_2O)_2(HPO_4)_2(C_2O_4)]\cdot H_2O$, reported by Rao and co-workers.[17] Interestingly this material contains no amine despite the presence of cyclohexylamine in the synthesis mixture. As a consequence of the absence of a charge balancing species, the iron is found in the 3+ oxidation state. The channels in $[Fe_2(H_2O)_2(HPO_4)_2(C_2O_4)]\cdot H_2O$ contain water molecules only. The connectivity around the iron atom

Table 4 Comparison of channel sizes in [SDA][$Mn_2(HPO_4)_2(C_2O_4)(H_2O)_2$] and $[Fe_2(H_2O)_2(HPO_4)_2(C_2O_4)]\cdot H_2O$[17] where SDA = $H_3NC_6H_{10}NH_3$ (**1**), $H_3N(CH_2)_2NH_3$ (**2**) and $H_3N(CH_2)_3NH_3$[10]

SDA	Oxalate–oxalate cross channel distance[a]/Å	Metal–metal cross channel distance[b]/Å
$H_3NC_6H_{10}NH_3$ (**1**)	8.466	10.79
$H_3N(CH_2)_2NH_3$ (**2**)	8.965	11.24
$H_3N(CH_2)_3NH_3$	9.056	10.45
$[Fe_2(H_2O)_2(HPO_4)_2(C_2O_4)]\cdot H_2O$	7.342	13.34

[a] From the midpoint of one C–C bond to the next. This is equivalent to the unit cell parameter *c* in **1**, $[H_3N(CH_2)_3NH_3][Mn_2(HPO_4)_2(C_2O_4)(H_2O)_2]$ and $[Fe_2(H_2O)_2(HPO_4)_2(C_2O_4)]\cdot H_2O$, *b* in **2**. [b] From the metal at the top of the channel to that opposite, parallel to *b* in **1**, $[H_3N(CH_2)_3NH_3][Mn_2(HPO_4)_2(C_2O_4)(H_2O)_2]$ and $[Fe_2(H_2O)_2(HPO_4)_2(C_2O_4)]\cdot H_2O$, *c* in **2**.

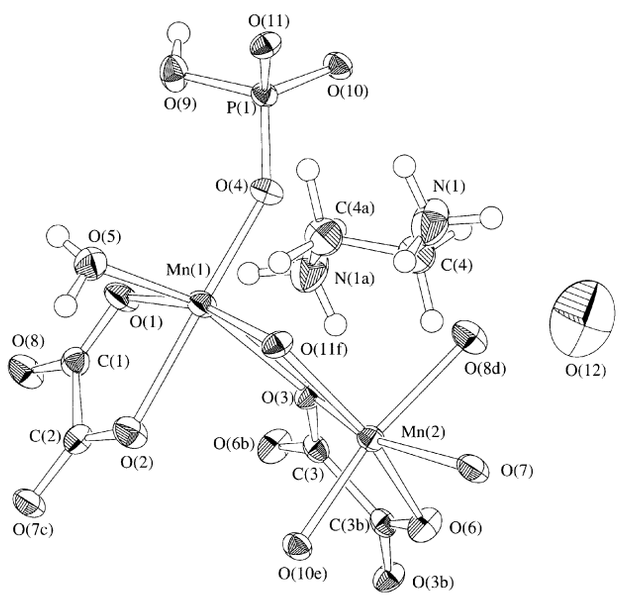

Fig. 6 Building unit of $[H_3N(CH_2)_2NH_3][Mn_4(HPO_4)_2(C_2O_4)_3(H_2O)_2]\cdot 2H_2O$ **3** showing the atom labelling scheme. Ellipsoids are shown at 50% probability. Symmetry labels: a, $-x+2$, $-y-1$, $-z+2$; b, $-x+2$, $-y-2$, $-z+2$; c, $x+1$, y, z; d, $x-1$, y, z; e, x, $y-1$, z; f, $-x+2$, $-y-1$, $-z+1$.

corresponds to that of **2** in Fig. 5, rather than that of **1**. A comparison of the channel sizes in all three materials (containing diaminopropane, ethylenediamine and diaminocyclohexane) together with the 'untemplated' iron(III) phase[17] is given in Table 4.

$[H_3N(CH_2)_2NH_3][Mn_4(HPO_4)_2(C_2O_4)_3(H_2O)_2]\cdot 2H_2O$ 3. Reaction of the same manganese–phosphate–oxalate hydrate mixture with ethylenediamine rather than *trans*-1,4-diaminocyclohexane produces mainly $[H_3N(CH_2)_2NH_3][Mn_4(HPO_4)_2(C_2O_4)_3(H_2O)_2]\cdot 2H_2O$ **3**, which has a very different composition and a more complex 3-D structure than **1** and **2**. This structure is built from edge-sharing MnO_6 octahedra and two crystallographically different types of oxalate anion. Two independent manganese cations are present in the structure, both adopting distorted octahedral co-ordination. The building unit is shown in Fig. 6; selected bond lengths and angles are in Table 5.

Bond valence sums give 2.03 for Mn(1) and 2.06 for Mn(2). Calculations for O(5) (0.32) and O(9) (1.10) indicate the presence of H_2O on Mn(1) and OH on P(1) respectively.

Mn(1) and Mn(2) share an edge through a phosphate and an oxalate oxygen (O(11) and O(3), respectively), both O atoms therefore being three-co-ordinate. These dimeric units share corners with HPO_4 tetrahedra, forming chains in the *b* direction

Table 5 Selected bond lengths (Å) and angles (°) in $[H_3N(CH_2)_2NH_3][Mn_4(HPO_4)_2(C_2O_4)_3(H_2O)_2]\cdot 2H_2O$ **3**

Mn(1)–O(1)	2.205(3)	Mn(2)–O(3)	2.246(3)
Mn(1)–O(2)	2.258(3)	Mn(2)–O(6)	2.242(3)
Mn(1)–O(3)	2.362(3)	Mn(2)–O(7)	2.237(4)
Mn(1)–O(4)	2.045(3)	Mn(2)–O(8)	2.186(3)
Mn(1)–O(5)	2.208(4)	Mn(2)–O(10)	2.076(3)
Mn(1)–O(11)	2.144(3)	Mn(2)–O(11)	2.158(3)
O(1)–Mn(1)–O(2)	74.1(1)	O(3)–Mn(2)–O(6)	73.7(1)
O(1)–Mn(1)–O(3)	95.5(1)	O(3)–Mn(2)–O(7)	159.9(1)
O(1)–Mn(1)–O(4)	92.6(1)	O(3)–Mn(2)–O(8)	89.0(1)
O(1)–Mn(1)–O(5)	92.0(2)	O(3)–Mn(2)–O(10)	104.0(1)
O(1)–Mn(1)–O(11)	166.0(1)	O(3)–Mn(2)–O(11)	78.3(1)
O(2)–Mn(1)–O(3)	78.7(1)	O(6)–Mn(2)–O(7)	96.1(1)
O(2)–Mn(1)–O(4)	163.9(1)	O(6)–Mn(2)–O(8)	95.4(1)
O(2)–Mn(1)–O(5)	84.8(1)	O(6)–Mn(2)–O(10)	85.0(1)
O(2)–Mn(1)–O(11)	93.0(1)	O(6)–Mn(2)–O(11)	151.2(1)
O(3)–Mn(1)–O(4)	93.8(1)	O(7)–Mn(2)–O(8)	74.4(1)
O(3)–Mn(1)–O(5)	159.3(1)	O(7)–Mn(2)–O(10)	92.1(1)
O(3)–Mn(1)–O(11)	76.0(1)	O(7)–Mn(2)–O(11)	112.7(1)
O(4)–Mn(1)–O(5)	105.1(2)	O(8)–Mn(2)–O(10)	166.5(1)
O(4)–Mn(1)–O(11)	99.1(1)	O(8)–Mn(2)–O(11)	91.0(1)
O(5)–Mn(1)–O(11)	92.5(1)	O(10)–Mn(2)–O(11)	95.0(1)

A	H	B	A–H	H···B	A···B	A–H···B
O(5)	H(1)	O(1)	0.69(7)	2.21(7)	2.887(6)	167(8)
O(5)	H(2)	O(7)	0.87(7)	2.02(7)	2.868(5)	166(6)
N(1)	H(3)	O(10)	0.95	1.86	2.797(6)	172
N(1)	H(4)	O(12)	0.95	2.07	2.901(6)	147
N(1)	H(5)	O(8)	0.95	2.44	3.147(6)	130
O(5)	H(1)	O(9)	0.69(7)	2.94(7)	3.194(6)	105(6)
N(1)	H(3)	O(4)	0.95	2.46	2.881(6)	107

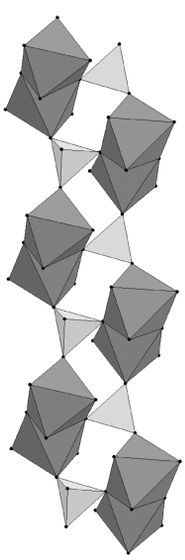

Fig. 7 A chain in **3** running parallel to the *b* axis. MnO_6 dark grey octahedra, PO_4 light grey tetrahedra.

containing eight-membered rings (see Fig. 7). These chains are linked in both the *a* and *c* directions by oxalate anions to form a 3-D network, illustrated in Figs. 8 and 9. As seen in Fig. 9, channels are created in the *a* direction, where diprotonated ethylenediamine cations and water molecules reside.

Interestingly this structure contains two different types of water; $O(5)H_2$ is a ligand on Mn(1), whilst $O(12)H_2$ is an unco-ordinated molecule within the channel space. An iron-containing material, $[N_2C_4H_{12}][Fe_4(HPO_4)_2(C_2O_4)_3]$, which is similar to **3** has been reported by Rao and co-workers.[18] This contains a different cation, piperazine, and no water molecules either in the channels or as ligands, resulting in a five-co-ordinate Fe atom. Replacing ethylenediamine by piperazine in the synthesis of **3** did result in the formation of a product with

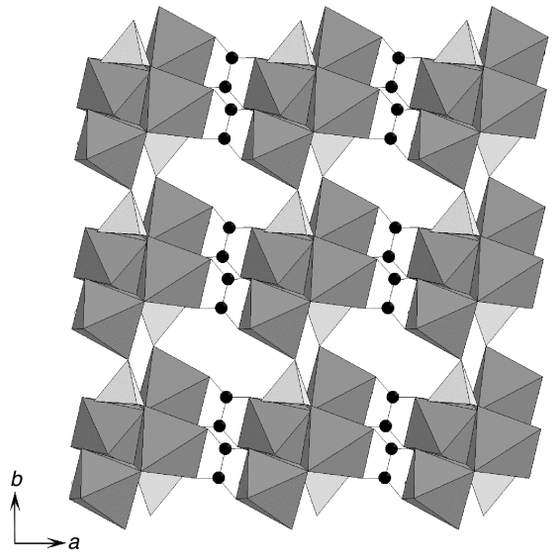

Fig. 8 *ab* projection of **3** showing oxalate anions connecting manganese phosphate chains in the *a* direction. MnO_6 dark grey octahedra, PO_4 light grey tetrahedra, C black.

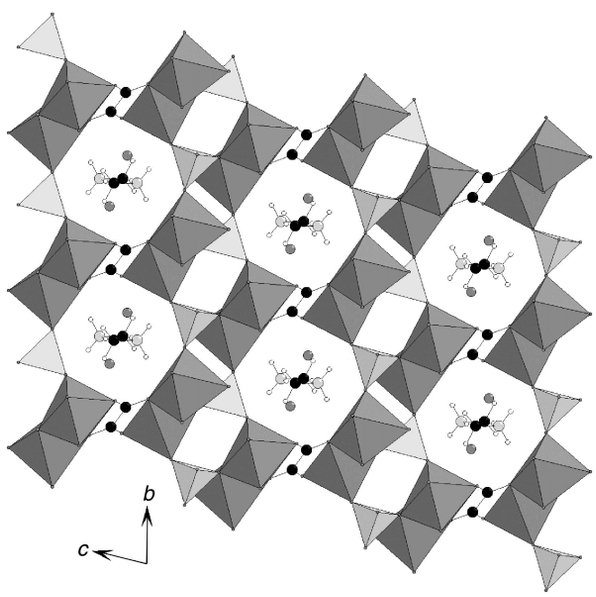

Fig. 9 *bc* projection of **3** with oxalate anions connecting manganese phosphate chains in the *c* direction, and cations and water in the *a* channels. MnO_6 dark grey octahedra, PO_4 light grey tetrahedra, C black, N light grey, H white.

a similar powder pattern to that of **3**, with a triclinic cell ($P\bar{1}$), with unit cell parameters 7.814(3), 8.098(2), 9.762(4) Å; 75.89(2), 79.07(2) and 86.72(2)°. Structure solution with the data set obtained has so far not been possible, however it would appear that the manganese phosphate oxalate framework of **3** can form in the presence of both ethylenediamine and piperazine.

Thermogravimetric analysis

$[H_3NC_6H_{10}NH_3][Mn_2(HPO_4)_2(C_2O_4)(H_2O)_2]$. Two small weight losses occur when heating **1** under O_2; 0.67% starting at 36 °C, and a further 1.53% to 180 °C. A sample heated to 180 °C and exposed to air when cooled was also identified as the starting material. A large, relatively sudden weight loss of 49.15% at 300 °C gives $Mn_2P_2O_7$ and Mn_2O_3 (JCPDS 29-891 and 24-508). The N_2 trace follows a very similar path, apart from a large exotherm which occurs under O_2 around 400 °C. The final losses at 800 °C are 54.36 (N_2) and 52.34% (O_2).

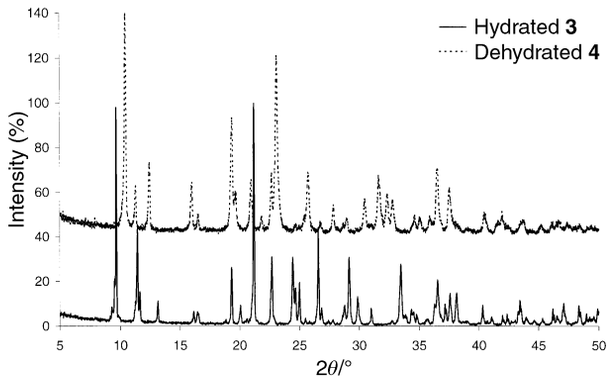

Fig. 10 Powder X-ray diffraction patterns of $[H_3N(CH_2)_2NH_3][Mn_4(HPO_4)_2(C_2O_4)_3(H_2O)_2]\cdot 2H_2O$ **3** and its dehydrated form **4**.

Both losses are endothermic under N_2; the final product appears the same as under O_2 by powder X-ray diffraction. Loss of C_2O_4, $2H_2O$ and $H_2NC_6H_{10}NH_2$ from **1** is 43.95% weight.

$[H_3N(CH_2)_2NH_3][Mn_4(HPO_4)_2(C_2O_4)_3(H_2O)_2]\cdot 2H_2O$. Heated under O_2, **3** undergoes an endothermic loss between 150 and 200 °C of 7.74%. A sample heated to 225 °C and exposed to air gave a different phase, as yet not fully characterised. We believe this is a dehydration product (**4**), involving loss of the water ligand on one MnO_6 octahedron (calc. $2H_2O$ 4.45, $4H_2O$ 8.90%). This would result in a five-co-ordinate species, and would be similar to the phase $[N_2C_4H_{12}][Fe_4(HPO_4)_2(C_2O_4)_3]$ reported by Rao and co-workers.[18] The powder diffraction patterns of **3** and **4** are shown in Fig. 10. Indexing of **4** gave a monoclinic cell of $a = 7.906$, $b = 7.881$, $c = 17.071$ Å and $\beta = 94.52°$. This compares with values of 7.569(2), 7.821(2), 18.033(4) Å and 98.8(1)° for $[N_2C_4H_{12}][Fe_4(HPO_4)_2(C_2O_4)_3]$ in space group $P2_1/c$. Structure refinement of **4** using $[N_2C_4H_{12}][Fe_4(HPO_4)_2(C_2O_4)_3]$ as a starting model has so far proved unsatisfactory, apparently due to preferred orientation problems.

Above 300 °C, two further losses occur, of 27.66 and 2.35%, both exothermic. The final product at 600 °C is largely amorphous, possibly containing Mn_2O_3 (JCPDS 24-508).

The N_2 and O_2 plots again follow a similar path, the N_2 being a more simple two step process, both endothermic. The total losses at 600 °C are 42.68 (O_2) and 40.25% (N_2). The final product after heating with N_2 is thought to be $Mn_3(PO_4)_2$ (JCPDS 33-901). For **3**, loss of $3C_2O_4$, $4H_2O$ and $H_2N(CH_2)_2NH_2$ is 48.92%.

Magnetic measurements

Magnetisation data were corrected for the diamagnetism of the constituent atoms and converted into molar susceptibility. In all cases field-cooled data were indistinguishable from zero-field cooled data. Plots of susceptibility and effective magnetic moment against temperature are shown in Fig. 11. **1**, **3** and **4** show antiferromagnetic behaviour, with clear maxima in the susceptibility curves at 7, 10 and 12 K respectively. The room temperature effective magnetic moment per Mn of the samples **1**, **3** and **4** is 5.67, 5.68 and 5.69 μ_B respectively. The lower than spin-only values of the moment and maxima in susceptibility curves indicate the presence of antiferromagnetic interactions. Therefore, the molar susceptibility χ_m over the temperature range 100–300 K was fitted by a Curie–Weiss model, $\chi_m = C/(T - \theta)$. The parameter minimised in the fitting process was R, where $R = (1/n)\,\Sigma\,(|\chi_{calc} - \chi_{obs}|)/(T\chi_{calc})$ and χ_{calc} and χ_{obs} are the calculated and observed molar susceptibilities respectively, n is the total number of data points, and T the temperature of measurement. The best fits obtained for the three compounds yielded $C = 4.235$ emu K mol^{-1}, $\theta = -15.6$ K, $R = 8.33 \times 10^{-4}$ for **1**, $C = 4.282$ emu K mol^{-1}, $\theta = -17.7$ K, $R = 6.83 \times 10^{-4}$ for **3**, and $C = 4.393$ emu K mol^{-1}, $\theta = -25.1$ K, $R = 11.16 \times 10^{-4}$ for **4**. In addition, the data were also fitted for $S = 5/2$ Bleaney–Bowers dimers in a mean field according to the equation $\chi_m = Cf1/f2$ where $C = Ng^2\mu_B{}^2/k(T - \theta)$, $f1 = 2\exp(2x) + 10\exp(6x) + 28\exp(12x) + 60\exp(20x) + 110\exp(30x)$, $f2 = 1 + 3\exp(2x) + 5\exp(6x) + 7\exp(12x) + 9\exp(20x) + 11\exp(30x)$, and $x = J/kT$.[19] The best fits obtained in this case were as follows: for **1**, $g = 1.97$, $J = 0.245$ K, $\theta = -14.3$ K, $R = 1.36 \times 10^{-3}$; for **3**, $g = 1.99$, $J = 0.476$ K, $\theta = -16.3$ K, $R = 5.85 \times 10^{-3}$; and for **4**, $g = 2.00$, $J = 0.62$ K, $\theta = -20.3$ K and $R = 1.71 \times 10^{-2}$. Inclusion of the possibility of the presence of monomeric manganese impurities did not increase the quality of the fits appreciably. It was not possible to obtain good fits to the data for large ratios of $J : \theta$ so it would appear that the susceptibility is not well described by a $S = 5/2$ dimer model, but rather by a simple mean-field model.

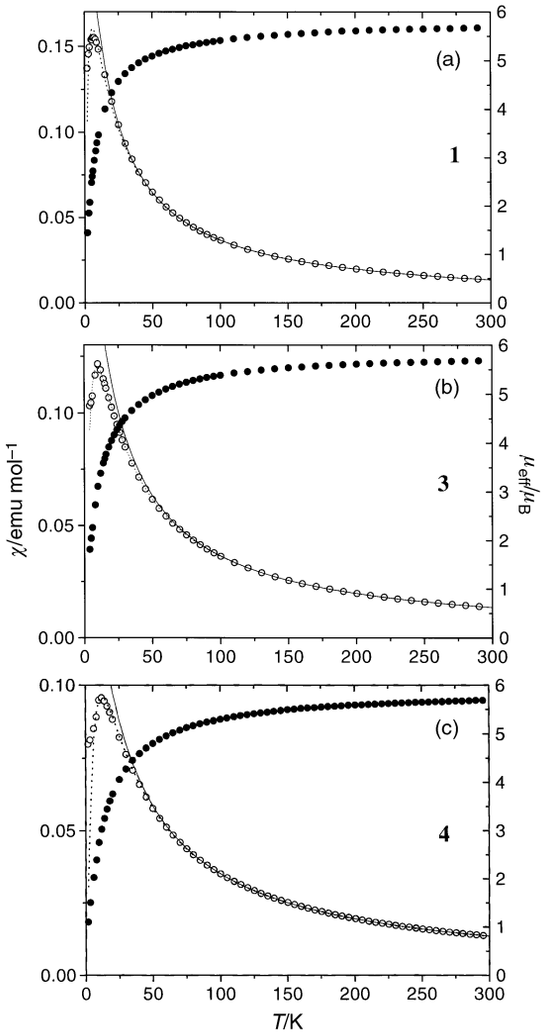

Fig. 11 Susceptibility (open circles) and effective magnetic moment (closed circles) *versus* temperature for $[H_3NC_6H_{10}NH_3][Mn_2(HPO_4)_2(C_2O_4)(H_2O)_2]$ **1** (*a*), $[H_3N(CH_2)_2NH_3][Mn_4(HPO_4)_2(C_2O_4)_3(H_2O)_2]\cdot 2H_2O$ **3** (*b*) and its dehydrated form **4** (*c*). In all graphs, the best fits by a Curie–Weiss expression are denoted by a continuous line, while the best fit by an $S = 5/2$ Bleaney–Bowers expression with mean-field coupling between the dimers is denoted by a dotted line.

Discussion and conclusion

Three new three-dimensional manganese phosphate oxalate materials have been synthesized hydrothermally. $[H_3NC_6H_{10}NH_3][Mn_2(HPO_4)_2(C_2O_4)(H_2O)_2]$ **1** and $[H_3N(CH_2)_2NH_3][Mn_2(HPO_4)_2(C_2O_4)(H_2O)_2]$ **2** consist of manganese phosphate layers which are pillared by oxalate anions, and contain one-

dimensional channels where diprotonated *trans*-1,4-diaminocyclohexane or ethylenediamine cations are found. Similar structures have been synthesized using diaminopropane,[10] and an iron-containing framework with no amine has been reported.[17] It is interesting that, while the use of different templates in the manganese(II) system modifies the structure, with Fe(III) the framework forms without an amine (despite the presence of cyclohexylamine in the synthesis mixture). $[H_3N(CH_2)_2NH_3][Mn_4(HPO_4)_2(C_2O_4)_3(H_2O)_2]\cdot 2H_2O$ **3** is constructed from edge-sharing MnO_6 dimers, which are connected by PO_4 groups into chains. Oxalate anions connect the chains in two directions to form the 3-D structure. Upon heating, a new phase (**4**) is formed which is believed to be a dehydrated form. It is apparent, from relationships between the lattice parameters, that this phase is related to a known Fe-containing material which contains Fe in both six- and five-fold co-ordination. This implies that the dehydration of **3** to **4** involves loss of both co-ordinated and unco-ordinated water, with a reduction of co-ordination from six to five for one Mn. This phase does not appear to rehydrate on standing at ambient temperature in moist air. Further work is required fully to solve this structure. It is known that the presence of 'zeolitic' water may also influence the magnetic properties of materials of this type. Cheetham, Férey and co-workers have reported a nickel phosphonate which undergoes two dehydration steps whilst retaining much of the original structure.[20] $Ni_4(O_3PCH_2PO_3)_2(H_2O)_3$ (VSB-2) is a layered material, with four octahedral Ni atoms. Loss of one H_2O from the formula gives VSB-3, which is three-dimensional and contains three nickel octahedra and one tetrahedron. The remaining two waters are removed by further heating, giving VSB-4 (also 3-D), with one nickel octahedron, one tetrahedron and three square pyramids. It is thought that these changes in the co-ordination of the nickel are responsible for the differences in magnetic properties of the three materials. VSB-3 has a much higher magnetisation (at 100 G) and shows hard ferromagnetic behaviour, whereas VSB-2 and VSB-4 are canted ferromagnets. A further example is the fluorinated iron phosphate framework, ULM-12, which can also be dehydrated leading to a change in the iron(II) co-ordination polyhedra.[21] $[N_2C_6H_{14}][Fe_4(PO_4)_4F_3(H_2O)_3]$ (ULM-12) loses three water molecules to form ULM-19 (a canted antiferromagnet), resulting in the formation of new six-membered rings. ULM-12 has a Neel temperature of 11 K, while that of ULM-19 is 9 K. The θ_p/T_N value, which is a measure of frustration in the system, is higher for ULM-19 (25) than ULM-12 (10). In the present case, dehydration of **3** to **4** results in a modest change of antiferromagnetic interactions (see above).

In summary, this work illustrates once again the rich variety of new materials to be obtained from complex hydrothermal systems. It appears that some frameworks, such as those of **2**, $[H_3N(CH_2)_3NH_3][Mn_2(HPO_4)_2(C_2O_4)(H_2O)_2]$[10] and $[Fe_2(H_2O)_2(HPO_4)_2(C_2O_4)]\cdot H_2O$,[17] can form with or without structure-directing agents, whereas that adopted by **1** has so far only been observed for the $[H_3NC_6H_{10}NH_3]^{2+}$-containing phase. Moreover, the basic building units within these compositions are essentially the same, but their mode of linkage in the final product is subtly dependent on the conditions and SDA used. We have also seen, in phase **3** and its analogue $[N_2C_4H_{12}][Fe_4(HPO_4)_2(C_2O_4)_3]$,[18] that essentially the same framework can be obtained with or without co-ordinated and extra-framework water and, apparently, that this water can be removed topotactically in a post-synthesis treatment. This dehydration has subtle influences on the magnetic behaviour of the material, and will possibly have more dramatic influence in certain situations, for example if mixed metal analogues (*e.g.* Mn(II)/Cu(II)) can be made, where the two magnetically active cations have different co-ordination preferences and order on different crystallographic sites. Interesting behaviour of this type has been observed, for example, in the 1-D chain material $[MnCu(pbaOH)(H_2O)_3]\cdot 2H_2O$ (pbaOH = 1,3-trimethylenebis(oxamate)).[22] Attempts to prepare mixed metal analogues of our phases are in progress.

Acknowledgements

We thank Dr A. M. Z. Slawin for collection of the X-ray diffraction data, and the EPSRC for funding.

References

1 A. K. Cheetham, G. Férey and T. Loiseau, *Angew. Chem.*, *Int. Ed.*, 1999, **38**, 3268.
2 R. Pellaux, H. W. Schmalle, R. Huber, P. Fischer, T. Hauss, B. Ouladdiaf and S. Decurtins, *Inorg. Chem.*, 1997, **36**, 2301.
3 C. J. Nuttall and P. Day, *Chem. Mater.*, 1998, **10**, 3050.
4 C. Mathonière, C. J. Nuttall, S. G. Carling and P. Day, *Inorg. Chem.*, 1996, **35**, 1201.
5 S. Decurtins, H. W. Schmalle, H. R. Oswald, A. Linden, J. Ensling, P. Gutlich and A. Hauser, *Inorg. Chim. Acta*, 1994, **216**, 65.
6 E. Coronado, J.-R. Galán-Mascarós, C. J. Gómez-García and J. M. Martínez-Agudo, *Adv. Mater.*, 1999, **11**, 558.
7 M. Clemente-León, E. Coronado, J.-R. Galán-Mascarós and C. J. Gómez-García, *Chem. Commun.*, 1997, 1727.
8 P. Lightfoot, Z. A. D. Lethbridge, R. E. Morris, D. S. Wragg, P. A. Wright, Å. Kvick and G. B. M. Vaughan, *J. Solid State Chem.*, 1999, **143**, 74.
9 Z. A. D. Lethbridge and P. Lightfoot, *J. Solid State Chem.*, 1999, **143**, 58.
10 Z. A. D. Lethbridge, A. D. Hillier, R. Cywinski and P. Lightfoot, *J. Chem. Soc.*, *Dalton Trans.*, 2000, 1595.
11 A. Choudhury, S. Natarajan and C. N. R. Rao, *Chem. Mater.*, 1999, **11**, 2316.
12 A. Choudhury and S. Natarajan, *J. Mater. Chem.*, 1999, **9**, 3113.
13 L.-C. Hung, H.-M. Kao and K.-H. Lii, *Chem. Mater.*, 2000, **12**, 2411.
14 A. Altomare, M. C. Burla, M. Camalli, M. Cascarano, C. Giacovazzo, A. Guyliardi and G. Polidori, *J. Appl. Crystallogr.*, 1993, **26**, 343.
15 TEXSAN, Crystal Structure Analysis Package, Molecular Structure Corporation, Houston, TX, 1992.
16 I. D. Brown and D. Altermatt, *Acta Crystallogr.*, *Sect. B*, 1985, **41**, 244.
17 A. Choudhury, S. Natarajan and C. N. R. Rao, *Chem. Eur. J.*, 2000, **6**, 1168.
18 A. Choudhury, S. Natarajan and C. N. R. Rao, *J. Solid State Chem.*, 1999, **146**, 538.
19 C. J. O'Connor, *Prog. Inorg. Chem.*, 1982, **29**, 203.
20 Q. Gao, N. Guillou, M. Nogues, A. K. Cheetham and G. Férey, *Chem. Mater.*, 1999, **11**, 2937.
21 M. Cavellec, J. M. Greneche and G. Férey, *Microporous Mesoporous Mater.*, 1998, **20**, 45.
22 O. Kahn, Y. Pei, M. Verdaguer, J. P. Renard and J. Sletten, *J. Am. Chem. Soc.*, 1988, **110**, 782.